Article

Metabolomic Properties of the Fluid from the Surgical Ligation After Breast-Conserving Therapy and Intraoperative Radiotherapy

Agnieszka Gdowicz-Kłosok *, Łukasz Boguszewicz, Agnieszka Skorupa, Mateusz Ciszek, Maria Turska-di Amico, Małgorzata Krześniak, Barbara Łasut-Szyszka, Maria Sokół, Jerzy Wydmański

Posted Date: 6 March 2026

doi: 10.20944/preprints202603.0491.v1

Keywords: breast cancer; intraoperative radiotherapy (IOXRT); wound fluid metabolomics; NMR spectroscopy; tumour microenvironment; breast-conserving therapy (BCT); metabolic biomarkers; multivariate analysis

 doi:10.20944/preprints202603.0491.v1

Article

Metabolomic Properties of the Fluid from the Surgical Ligation After Breast-Conserving Therapy and Intraoperative Radiotherapy

Agnieszka Gdowicz-Kłosok [1,*,†], Łukasz Boguszewicz [2,†], Agnieszka Skorupa [2], Mateusz Ciszek [2], Maria Turska-di Amico [3], Małgorzata Krześniak [1], Barbara Łasut –Szyszka [1], Maria Sokół [2] and Jerzy Wydmański [4]

[1] Center for Translational Research and Molecular Biology of Cancer, Maria Skłodowska-Curie National Research Institute of Oncology, Gliwice Branch, 44-101 Gliwice, Poland
[2] Medical Physics Department, Maria Skłodowska-Curie National Research Institute of Oncology, Gliwice Branch, 44-101 Gliwice, Poland
[3] II Department of Oncological Surgery, Maria Skłodowska-Curie National Research Institute of Oncology, Gliwice Branch, 44-101 Gliwice, Poland
[4] Radiotherapy Department, Maria Skłodowska-Curie National Research Institute of Oncology, Gliwice Branch, 44-101 Gliwice, Poland
* Correspondence: Agnieszka.gdowicz-klosok@gliwice.nio.gov.pl; Tel.: +48-32-278-96-38
† Equal contribution.

Abstract

Background: Intraoperative radiotherapy with low-energy X-rays (IOXRT) is an increasingly utilized modality during breast conserving therapy (BCT). However, the molecular mechanisms by which it affects the postoperative microenvironment remain to be fully elucidated. Surgical wound fluid (WF) has been demonstrated to modulate cancer cell behavior; however, its metabolomic composition has not been previously characterized in the context of breast cancer. The objective of this study was to evaluate metabolic alterations in postoperative WF and to determine whether IOXRT induces distinct metabolic signatures compared with mastectomy (AMP). **Methods:** Postoperative WF was collected from 54 breast cancer patients (38 BCT IOXRT; 16 AMP) at two time points: day 1 (A) and day 5 (B) after surgery. The samples were then subjected to analysis using ^{1}H NMR spectroscopy, encompassing NOESY, CPMG, and JRES techniques. A total of 114 spectral signals were quantified, and 42 metabolites were identified. Multivariate analyses (PCA, PLS DA, OPLS DA) and Wilcoxon signed rank tests were applied to assess temporal and intergroup differences. **Results:** A clear metabolic separation between time points A and B was observed in both treatment groups. However, statistical analysis revealed no significant differences between BCT IOXRT and AMP. In BCT IOXRT, on the fifth day, WF exhibited a decline in branched chain amino acids, asparagine, lysine, methionine, and glutamate, concomitant with an increase in lactate and pyruvate. AMP-specific alterations encompassed a decrease in 2-oxoglutarate and hypoxanthine on the first day, along with an increase in glucose and creatinine on the fifth day. A decline in ketone bodies (3-hydroxybutyrate, acetoacetate, acetone) was observed in both groups. **Conclusions:** Postoperative WF demonstrates dynamic metabolic changes reflecting early wound healing processes and treatment-related effects. IOXRT has been found to be associated with enhanced glycolytic signatures and reduced amino acid levels, suggesting altered metabolic activity in the irradiated tumor bed. The metabolomic profiling of WF has the potential to offer a novel source of biomarkers, which could facilitate the assessment of treatment response and tumor microenvironment characteristics.

Keywords: breast cancer; intraoperative radiotherapy (IOXRT); wound fluid metabolomics; NMR spectroscopy; tumour microenvironment; breast-conserving therapy (BCT); metabolic biomarkers; multivariate analysis

 doi:10.20944/preprints202603.0491.v1

Introduction

Breast cancer (BC) represents the most prevalent form of cancer among women worldwide, with an estimated 2.3 million new cases each year. Despite increased self-awareness and more effective methods for detecting and treating this cancer, the number of deaths from it remains high at nearly 700,000 per year (Bray et al., 2024). It is estimated that one in eight women will develop breast cancer at some point in their lives (Sung et al. 2021; Bray et al. 2024). Therefore, it is imperative to continue to look for increasingly effective methods to treat and prevent breast cancer.

Breast conservation therapy (BCT) represents the standard of care for patients with early-stage breast cancer. Initially used as a standalone intervention, surgical treatment was found to be associated with a considerable risk of local recurrence (McCready et al., 1996).

Radiotherapy is a highly effective local treatment method, especially in the context of subclinical cancer foci in the tumour bed.

Therefore, it is important to consider areas with a high risk of cancer recurrence, such as the mammary gland, especially the stroma of the removed tumor and the regional lymphatic system. Postoperative radiotherapy has been shown to reduce the risk of local and regional recurrence. It has been shown to significantly reduce the risk of local recurrence of carcinoma in situ, as well as invasive cancer (Donker et al., 2013).

The use of radiotherapy during surgical procedures, called intraoperative radiotherapy (IORT), has the advantage of allowing for the delivery of a high dose to the breast tumour bed while sparing healthy tissue. This not only reduces the risk of radiation-induced injury but also may accelerate local healing (improving the therapeutic index).

Direct access to the surgical site markedly decreases the probability of geographic error and provides near certainty that the planned dose will be administered accurately in the area of greatest risk of local recurrence (Vaidya et al., 2001).

The use of IORT as a boost (additional dose in the tumour bed) is particularly important in the context of oncoplastic surgery, which is becoming more common due to better cosmetic effects. Identifying the tumour bed after this type of procedure is particularly challenging and carries a significant risk of geographic error. The use of X-rays radiation therapy (IOXRT)offers the advantage of sparing healthy tissue and organs due to the characteristics of the radiation used (its intensity rapidly decreases with depth) and its ability to separate and shield tissue from the high-dose area. IORT allows for the performance of surgery and radiotherapy in a single session, shortening the overall treatment time. In addition to favourable therapeutic and cosmetic outcomes, intraoperative radiotherapy offers significant economic and logistical advantages (Pilar A et al., 2017). In randomized clinical trial, TARGIT-A, demonstrated high treatment efficacy with intraoperative radiotherapy, reduced treatment costs, and superior cosmetic results (Veronesi et al. 2013, Vaidya et al. 2014, Piroth et al. 2022). Surgical treatment has been shown to influence the process of metastasis and local recurrence. 1305 patients were randomised (654 to external radiotherapy and 651 to intraoperative radiotherapy) between Nov 20, 2000, and Dec 27, 2007. After a medium follow-up of 5·8 years (IQR 4·1-7·7), 35 patients in the intraoperative radiotherapy group and four patients in the external radiotherapy group had had an IBTR (p<0·0001). The 5-year event rate for IBRT was 4·4% (95% CI 2·7-6·1) in the intraoperative radiotherapy group and 0·4% (0·0-1·0) in the external radiotherapy group (hazard ratio 9·3 [95% CI 3·3-26·3]). During the same period, 34 women allocated to intraoperative radiotherapy and 31 to external radiotherapy died (p=0·59). 5-year overall survival was 96·8% (95% CI 95·3-98·3) in the intraoperative radiotherapy group and 96·9% (95·5-98·3) in the external radiotherapy group. In patients with data available (n=464 for intraoperative radiotherapy; n=412 for external radiotherapy) we noted significantly fewer skin side-effects in women in the intraoperative radiotherapy group than in those in the external radiotherapy group (p=0·0002).The underlying molecular mechanisms of these processes are poorly understood. The potential benefits of IORT, particularly IOXRT, warrant further investigation, not only in terms of its clinical utility but also in terms of its molecular mechanisms of action. Note that X-rays exhibit considerably higher

 doi:10.20944/preprints202603.0491.v1

relative biological efficiency (RBE) compared to megavoltage radiation. This effect is further amplified at lower radiation energies.

The direct and indirect effects of intraoperative radiation therapy (IORT) on the inhibition of local tumor recurrence.

Intraoperative radiotherapy (IORT) can influence the postoperative tumour bed through several interconnected biological mechanisms. Residual cancer cells that remain within the surgical cavity after tumour excision are exposed to a high single dose of radiation, which disrupts DNA repair pathways, promotes apoptotic signalling, and reduces proliferative and metastatic potential. Beyond these direct cytotoxic effects, IORT also modifies the local microenvironment by altering gene expression patterns, extracellular matrix organisation, and intercellular communication. Irradiated tumour cells may release damage-associated signals, exosomes, and tumour antigens that can be transported to regional lymphatic structures, contributing to systemic immune activation—a phenomenon consistent with the so-called abscopal effect (Figure 1, Jeibouei S et al., 2022). Surgical trauma itself is known to trigger inflammatory responses that can stimulate the growth of residual malignant cells; however, perioperative irradiation has been shown to counteract these pro-tumourigenic processes. Together, these observations highlight the complex interplay between surgical injury, radiation exposure, and immune modulation in shaping the risk of local recurrence(Belletti et al., 2008; Troester et al., 2009).

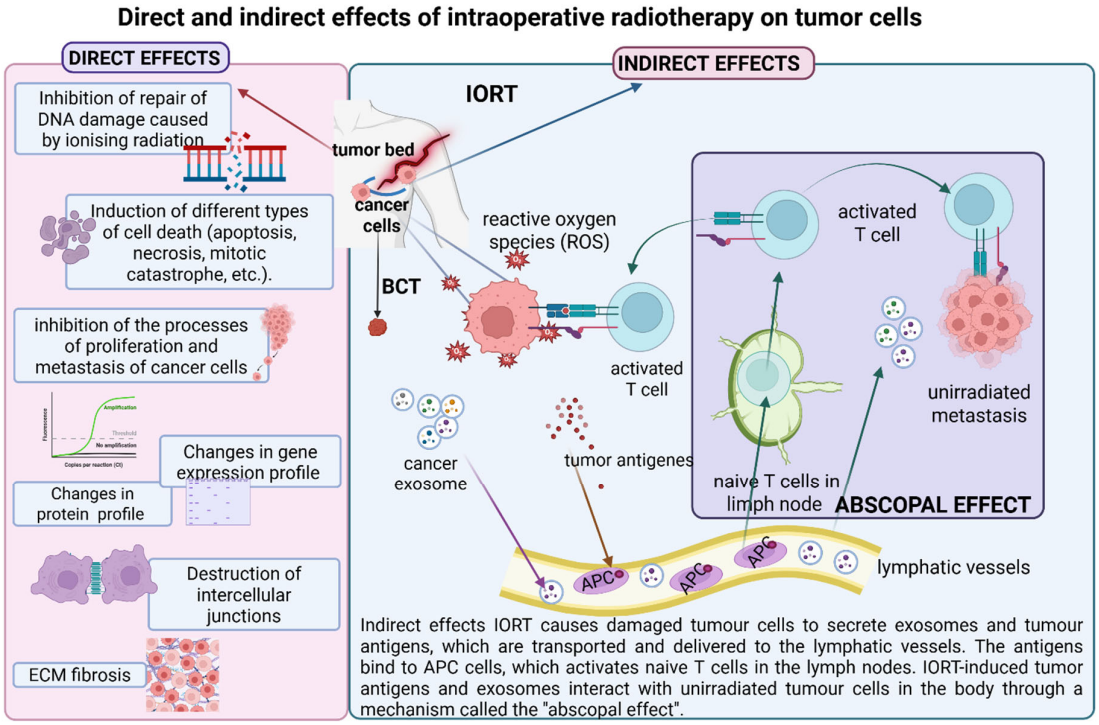

Figure 1. Direct and indirect effects of intraoperative radiotherapy on tumour cells. Own interpretation based on the publication Jeibouei S et al.2022, made in BioRender.

A more comprehensive understanding of the interaction between breast cancer cells and the tumour microenvironment in response to irradiation may facilitate the discovery of new treatment strategies for breast cancer. The existing literature indicates that surgical wound fluids (WF) collected from the surgical site after the removal of a breast tumor in vitro stimulate the growth, proliferation and invasiveness of breast cancer cells. Postoperative fluid collected from patients who received intraoperative radiotherapy was shown to exert markedly different effects on cancer cells compared to postoperative wound fluid from patients who underwent standard RT. Cells incubated with postoperative wound fluid after intraoperative radiotherapy (WF-IORT) exhibit a reduced

 doi:10.20944/preprints202603.0491.v1

population of cells with a stem-like phenotype (CD44 / CD24 / low) compared to cells incubated with postoperative fluid from patients undergoing standard radiotherapy (Zalewska et al., 2016). IORT has been shown to influence cancer cell biology by modulating microRNA (miRNA) levels, including miR-21, miR-155, and miR-221 (Zalewska et al., 2017). Postoperative fluid after IORT has been shown to induce the extrinsic apoptotic pathway in breast cancer cells, accompanied by an increase in the expression of genes involved in this pathway, including TNF, TRIAL, and CAS10 (Kulcenty et al., 2018). Furthermore, the use of IORT has been shown to induce an apoptotic effect and facilitate regression of distant metastatic foci (Jeibouei et al., 2022). Nuclear magnetic resonance (NMR) has also been used in the search for prognostic and predictive markers.

Nuclear magnetic resonance (NMR) in the search for prognostic and predictive biomarkers.

Nuclear magnetic resonance (NMR) spectroscopy has become a valuable tool in metabolomics, providing insight into the relationship between metabolic profiles of tissues and biological fluids and the presence or progression of cancer. Furthermore, it is a promising approach to monitor treatment results (Giskeødegård et al., 2018; Silva et al., 2019; Boguszewicz et al., 2024, 2021). However, to our knowledge, postoperative fluid in BC has not been studied metabolically to date. However, recent work has confirmed that the metabolic composition of exudate is of great clinical importance (Junka et al. 2017, Bala et al. 2008). Modern spectroscopic techniques allow for the evaluation of almost all wound processes. When coupled with plasma and tissue metabolic studies and clinical data, these techniques may have significant translational implications.

The application of high-resolution magic-angle spinning (HR-MAS) NMR spectroscopy to BC samples enabled the quantification of approximately 40 metabolites through the use of a safe and non-destructive methodology that necessitates minimal sample preparation (Gogiashvili et al., 2019). As HR-MAS analyzes intact tissue, it offers the possibility of further characterization of the same sample using other omics methods or histopathology (Vignoli et al., 2021). Several studies have shown that HR-MAS is capable of differentiating between malignant and normal breast tissue, as well as between carcinoma in situ and infiltrating carcinoma (Chae et al., 2016). Recently, our group has used this methodology to elucidate the metabolic profiles of the epithelial and stromal compartments in breast tumors (Skorupa et al., 2023). Furthermore, the HR-MAS NMR approach has been used effectively for the metabolic characterization of breast cancer cell lines (Maria et al., 2015) and the detection of chemotherapy effects (Maria et al., 2017).

Boguszewicz and colleagues conducted a retrospective metabolomic study, demonstrating the usefulness of blood serum metabolomics in predicting the response to ICHT in HNSCC (Boguszewicz et al. 2024).

In summary, metabolic profiles have been shown to align with histopathological classification and tumour malignancy and possess the capacity to differentiate responsive and nonresponsive tumours at the molecular level. Given the wealth of information that postoperative fluid metabolome analysis can provide, the objective of this project was to investigate the impact of IOXRT on selected molecular markers of response in breast cancer patients, with the aim of identifying predictive metabolic markers. The use of breast-sparing surgery as a research model allows the study of the effects of radiation therapy on surrounding tissues, as well as the monitoring of molecular and immunological changes over time. The fluid recovered from the surgical site exhibits biological properties that require thorough investigation.

Materials and Methods

The study was carried out according to the plan presented in Figure 2.

 doi:10.20944/preprints202603.0491.v1

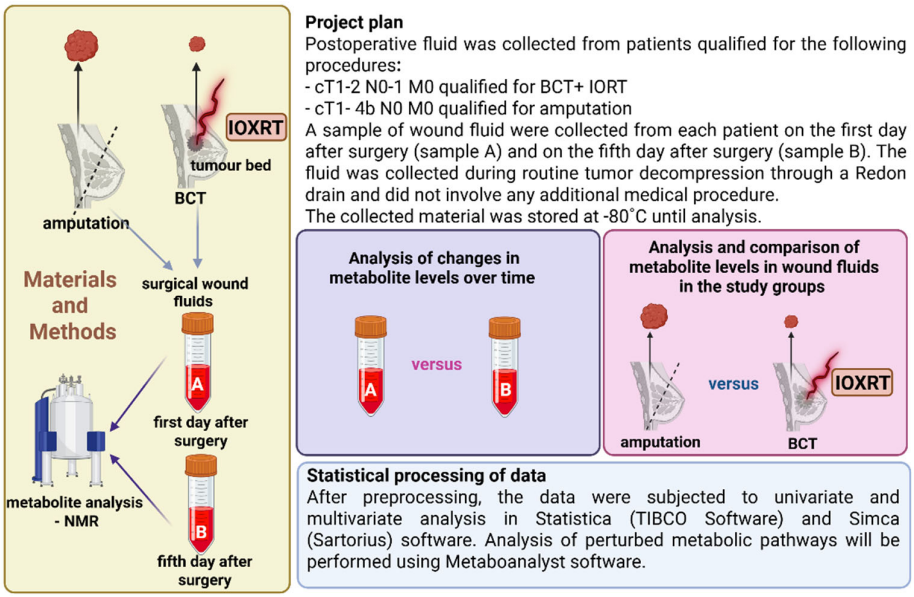

Figure 2. The workflow of the study (a scheme made using BioRender).

Population Study

Study Population

This prospective observational study was conducted at the National Institute of Oncology in Gliwice and received approval from the Ethics Committee of the National Institute of Oncology in Warsaw (decision No. 18/2024). All participants provided written informed consent. The study enrolled 54 women diagnosed with breast cancer: 38 treated with breast-conserving therapy combined with intraoperative X-ray radiotherapy (BCT-IOXRT) and 16 undergoing mastectomy.

The IOXRT procedure followed the technique previously described by Wydmański et al. (2005).

Postoperative wound fluid (WF) was collected at two predefined time points:

A — the first postoperative day,

B — the fifth postoperative day.

Each patient contributed two samples (A and B), except for one individual in the BCT-IOXRT group who underwent bilateral surgery and provided four samples. The timing of collection corresponded to standard clinical follow-up visits, minimizing the risk of sample loss. Clinical and pathological characteristics of the cohort are summarized in Table 1.

Table 1. Characteristics of the study population.

number of patients (n) 54			
age	66 (43-84)		
	BCT-IOXRT	38	5Gy – 35 10Gy - 3
	amputation	16	
grade	G0	1	2%
	G1	20	37%
	G2	28	52%
	G3	5	9%
T-stage	T0	34	63%
	T1	16	30%
	T2	3	6%
	T3	1	2%
N-stage	N0	52	96%
	N1	2	4%

 doi:10.20944/preprints202603.0491.v1

receptors status	ER positive	49	91%
	PR positive	42	78%
	HER2 positive	6	11%
Ki-67	≤ 15%	36	67%
	16-30%	12	22%
	>30%	6	11%

Processing of wound fluid samples

Immediately after collection, WF samples were centrifuged for clarification. The supernatant was sequentially passed through filters of decreasing pore size to remove cellular debris and particulate matter. The clarified fluid was aliquoted and stored at −80°C until further analysis.

This workflow follows the general approach routinely applied in our metabolomics laboratory and previously reported in Boguszewicz et al. (2023).

Preparation of samples for NMR spectroscopy

Before analysis, frozen WF aliquots were thawed gradually (first at 4°C, then at room temperature). Each sample was mixed with phosphate buffer (pH 7.4) containing D_2O for field locking and TSP as a chemical shift reference. A final volume of 600 µL was transferred into 5-mm NMR tubes and kept at 4°C until measurement.

The preparation strategy is consistent with established protocols used in our earlier metabolomic studies (Boguszewicz et al., 2021; Boguszewicz et al., 2024).

NMR data acquisition

All spectra were acquired on a Bruker Avance III 400 MHz spectrometer equipped with a 5-mm PABBI probe. Instrument tuning, shimming, and pulse calibrations were performed individually for each sample. The temperature during acquisition was maintained at 310 K.

Three types of ^1H NMR experiments were recorded for each sample: NOESY 1D, CPMG,J-resolved (JRES).

These experiments provide complementary information on metabolite composition and relaxation properties. The measurement scheme was adapted from the widely used protocol of Beckonert et al. (2007) and from procedures optimized in our laboratory (Boguszewicz et al., 2021; 2024).

Spectral processing and metabolite quantification

Spectra were processed using standard routines: exponential line broadening, automatic phase correction, and referencing to the formate peak at 8.47 ppm. Quantification was performed using the positive projections of JRES spectra. Integration regions were defined individually for each metabolite, and the resulting values were normalized to the total spectral area (9.0–0.5 ppm), excluding the water resonance region.

This analytical pipeline reflects the standard workflow applied in our metabolomics facility and described in Boguszewicz et al. (2023).

Metabolite identification

Metabolites were identified by comparing spectral features with reference libraries (Chenomx NMR Suite), chemical shift databases (HMDB), and published literature. Multiplicity patterns and scalar couplings from JRES spectra supported the assignments. In total, 114 NMR signals were quantified, of which 42 metabolites were confidently identified, several were annotated as probable, and a subset remained unassigned.

Statistical analysis

Multivariate statistical analyses were performed using SIMCA (v.18). Prior to modeling, variables were mean-centered and scaled to unit variance.

- PCA was used to explore variance structure.
- PLS-DA and OPLS-DA were applied for supervised discrimination.
- Model significance was evaluated using permutation testing and cv-ANOVA.

Paired comparisons between time points A and B were assessed using the Wilcoxon signed-rank test (Statistica v.12), with significance set at $p < 0.05$.

 doi:10.20944/preprints202603.0491.v1

Note on methodological overlap

All experimental procedures described above are standard protocols routinely used in our metabolomics laboratory and were originally developed and published by our team. To ensure transparency, the relevant methodological foundations are explicitly acknowledged through citations to Boguszewicz et al. (2023), as requested by the Editor.

Results

Assessment of the Variance Distribution in the Data

Figure 3 shows the results of the unsupervised PCA analyzes. A clear separation between time points A and B is visible in the whole study group (Figure 3 a), as well as separately in the BCT-IOXRT and AMP subgroups (Figure 3 b and c). However, the difference between the BCT-IOXRT and AMP subgroups is negligible (Figure 3 a, d, and e).

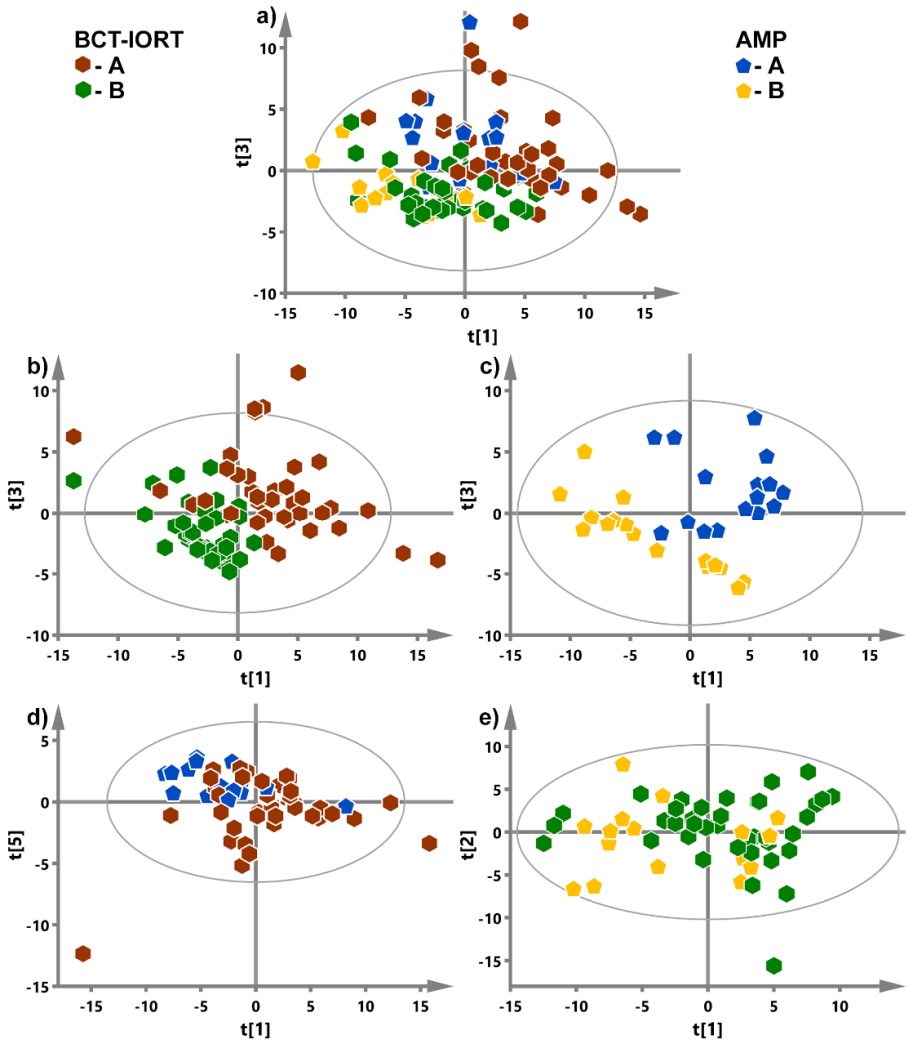

Figure 3. Score plots from PCA analyses. a – the study group, b – A and B time points in the BCT-IOXRT subgroup, c – A and B time points in the AMP subgroup, d – A time points in the BCT-IOXRT and AMP subgroups, e – B time points in the BCT-IOXRT and AMP subgroups.

 doi:10.20944/preprints202603.0491.v1

Class Separation and Identification of Important Variables

The supervised PLS-DA model was used to separate four classes: Time points A and B of the BCT-IOXRT and AMP subgroups, respectively. Four OPLS-DA models were used for two-class discrimination tasks: BCT-IOXRT A vs B and AMP A vs B as well as BCT-IOXRT vs AMP at time points A and B, respectively. The models distinguishing BCT-IOXRT from AMP (both time points A and B) did not meet the internal significance criteria, and thus these results are not presented. Table 2 shows the quality parameters of the significant models.

Table 2. Diagnostics of the PLS-DA and OPLS-DA models.

PLS-DA						
Component	R2X	R2Y	Q2			
1	0.21	0.218	0.199			
2	0.132	0.090	0.060			
3	0.154	0.044	0.008			
cv-ANOVA	0.000					
OPLS-DA						
	BCT-IOXRT A vs B			AMP A vs B		
Predictive component	R2X	R2Y	Q2	R2X	R2Y	Q2
1	0.134	0.844	0.699	0.151	0.909	0.615
Orthogonal component	R2X(o)			R2X(o)		
1	0.162			0.191		
2	0.073			0.059		
cv-ANOVA	0.000			0.000		

Figure 4 shows score plots of the PLS-DA (Figure 4 a) and OPLS-DA models (Figure 4 b and a c), and clear separation between A and B time points is visible in both PLS-DA and OPLS-DA. The important metabolites for class separation (with p(corr) > 0.3) were identified based on the SUS plot (Figure 3) combining the S plots of the BCT-IOXRT A vs. B and AMP A vs B OPLS-DA models. The statistical significance of the observed changes was assessed using the WSR test. The list of important metabolites with p(corr) values of p (corr) of OPLS-DA and values of p of the WSR test is presented in Table 3.

The SUS-plot (Figure 5) shows all quantified NMR signals as green squares. For metabolites with multiple signals in the NMR spectrum, all signals are included. Due to quantification uncertainty and/or due to overlap with other NMR signals, as well as because of significant difference in group size between BCT-IOXRT and AMP resonance signals of some metabolites (eg, valine) are shared between BCT-IOXRT and AMP (valine at 2.28 ppm) or unique for BCT-IOXRT (valine at 1.0 ppm, 1.05 ppm and 3.62 ppm) (Figure 5, Table 3). However, the trend of change between the A and B time points remains the same. Most NMR signals decrease from time point A to time point B. The increase is observed in the signals of methanol, unk/xanthine, lactate, pyruvate, glucose, creatinine and an unknown signal (Figure 5, Table 3).

 doi:10.20944/preprints202603.0491.v1

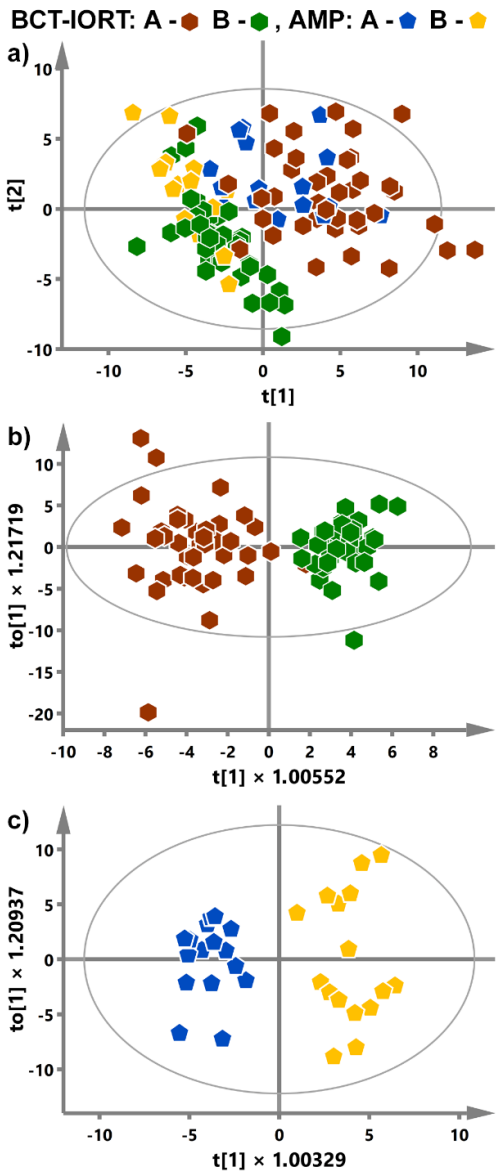

Figure 4. Score plots from the PLS-DA (a) and OPLS-DA (b and c) models. a - four-class discriminant model (PLS-DA), b – A vs B time points in the BCT-IOXRT subgroup (OPLS-DA), c – A vs B time points in the AMP subgroup (OPLS-DA).

 doi:10.20944/preprints202603.0491.v1

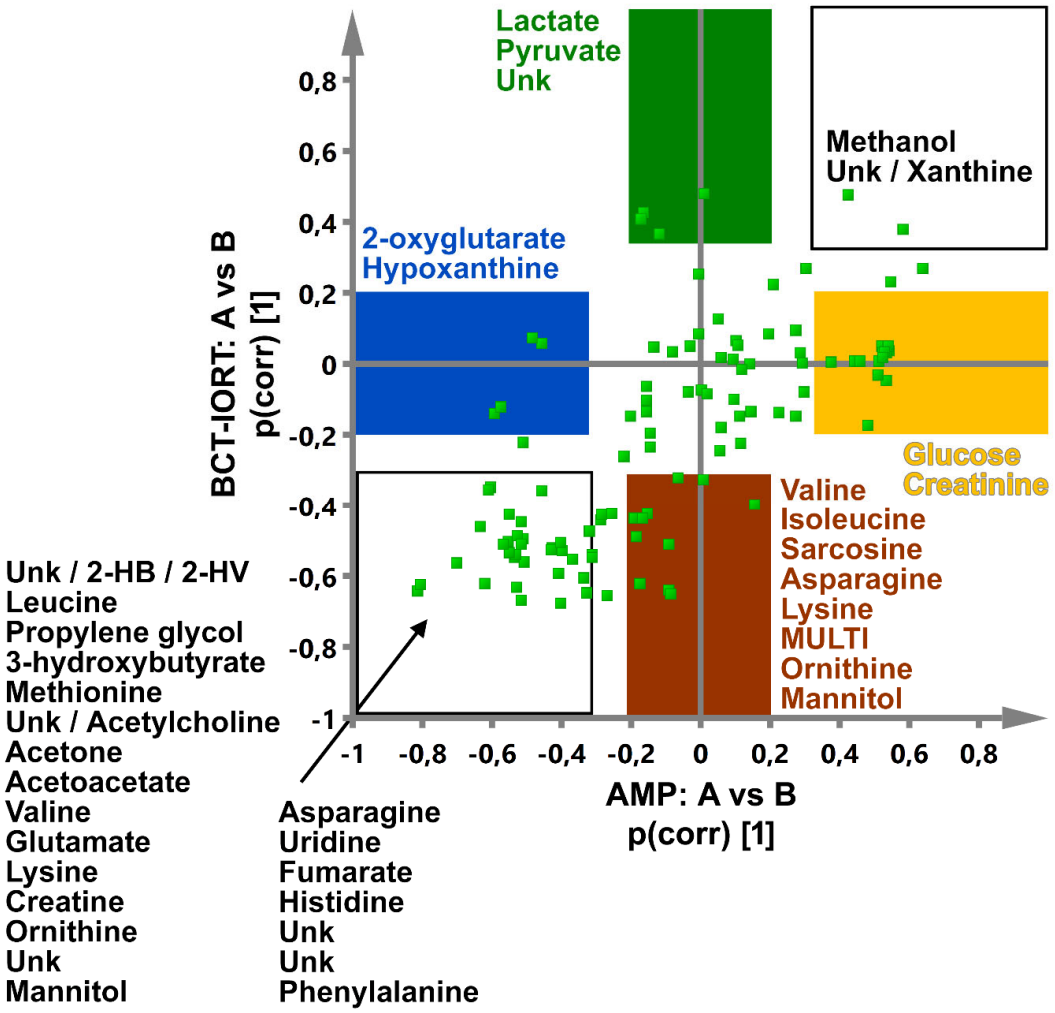

Figure 5. SUS-plot for OPLS-DA models distinguishing time points A and B in the BCT-IOXRT and AMP subgroups. Important metabolites (with p(corr) > 0.3) are indicated. Metabolites along the diagonal (inside the black squares) are shared between the BCT-IOXRT and AMP models. The metabolites outside the diagonal are unique for a specific model. Color coding corresponds to the colors used in Figures 4 and 5. Lower black square: the metabolites increased at time point A in both BCT-IOXRT and AMP. Upper black square: the metabolites increased at time point B in both BCT-IOXRT and AMP. Red rectangle: metabolites increased in the time point A of BCT-IOXRT. Green rectangle: the metabolites increased at time point B in BCT-IOXRT. Blue rectangle: the metabolites increased at time point A of AMP. Yellow rectangle: metabolites increased in the time point B of AMP. Unk: the unknown signal; MULTI: the overlapping signals of more than two metabolites; 2-HB – 2-hydroxybutyrate; 2-HV – 2-hydroxyvalerate.

Table 3. List of metabolites important for discrimination of A and B time points in BCT-IOXRT and AMP subgroups.

		BCT-IOXRT (A vs B)		AMP (A vs B)		Increase (↑) or decrease (↓) from A to B	
Metabolite	δ [ppm]	p(corr)	WSR p value	p(corr)	WSR p value	BCT-IOXRT	AMP
Metabolites unique for BCT-IOXRT (A)							
Valine	1.00	-0.42	0.000	-0.15	0.179	↓	
Valine	1.05	-0.44	0.000	-0.17	0.196	↓	
Valine	3.62	-0.49	0.000	-0.18	0.160	↓	

 doi:10.20944/preprints202603.0491.v1

Isoleucine	1.02	-0.44	0.000	-0.19	0.088	↓	
Sarcosine	2.76	-0.32	0.003	-0.07	0.836	↓	
Asparagine	2.89	-0.62	0.000	-0.17	0.234	↓	
Asparagine	2.95	-0.64	0.000	-0.09	0.110	↓	
Lysine	3.76	-0.65	0.000	-0.09	0.642	↓	
MULTI	3.77	-0.40	0.000	0.16	0.717	↓	
Ornithine	3.80	-0.33	0.004	0.01	0.408	↓	
Mannitol	3.82	-0.51	0.000	0.09	0.121	↓	
Metabolites unique for BCT-IOXRT (B)							
Lactate	1.34	0.43	0.000	-0.17	0.756	↑	
Lactate	4.13	0.41	0.000	-0.17	0.679	↑	
UNK	4.31	0.37	0.002	-0.12	0.535	↑	
Pyruvate	2.39	0.48	0.000	0.01	0.642	↑	
Metabolites unique for AMP (A)							
2-oxyglutarate	2.45	0.06	0.270	-0.46	0.026		↓
2-oxyglutarate	3.02	0.07	0.586	-0,48	0.017		↓
Hypoxanthine	8.19	-0.14	0.003	-0.59	0.003		↓
Hypoxanthine	8.21	-0.12	0.001	-0.57	0.003		↓
Metabolites unique for AMP (B)							
Glucose*	5.25	0.02	0.977	0.52	0.063		↑
Creatinine	4.07	0.01	0.890	0.38	0.039		↑
Metabolites shared between BCT-IOXRT (A) and AMP (A)							
Unk / 2-HB / 2-HV	0.91	-0.62	0.000	-0.62	0.001	↓	↓
Leucine	0.96	-0.53	0.000	-0.40	0.013	↓	↓
Leucine	0.97	-0.52	0.000	-0.43	0.008	↓	↓
Propylene glycol	1.15	-0.50	0.000	-0.55	0.009	↓	↓
3-hydroxybutyrate	1.21	-0.55	0.000	-0.53	0.000	↓	↓
3-hydroxybutyrate	2.32	-0.54	0.000	-0.53	0.000	↓	↓
3-hydroxybutyrate	2.42	-0.45	0.000	-0.52	0.000	↓	↓
3-hydroxybutyrate	4.17	-0.51	0.000	-0.52	0.001	↓	↓
Methionine	2.16	-0.67	0.000	-0.52	0.004	↓	↓
Methionine	2.66	-0.54	0.000	-0.31	0.063	↓	↓
Unk / Acetylcholine	2.18	-0.43	0.000	-0.55	0.003	↓	↓
Acetone	2.24	-0.46	0.000	-0.63	0.000	↓	↓
Acetoacetate	2.30	-0.53	0.000	-0.43	0.003	↓	↓
Valine	2.28	-0.56	0.000	-0.51	0.001	↓	↓
Glutamate	2.37	-0.63	0.000	-0.53	0.000	↓	↓
Lysine	3.04	-0.55	0.000	-0.37	0.070	↓	↓
Creatine	3.05	-0.50	0.000	-0.51	0.000	↓	↓
Creatine	3.95	-0.49	0.000	-0.53	0.001	↓	↓
Ornithine	3.08	-0.36	0.000	-0.46	0.010	↓	↓
Unk / Acetylcholine	3.20	-0.57	0.000	-0.70	0.000	↓	↓
Unk	3.37	-0.47	0.000	-0.32	0.022	↓	↓
Mannitol	3.70	-0.64	0.000	-0.81	0.000	↓	↓
Mannitol	3.89	-0.62	0.000	-0.81	0.001	↓	↓
Asparagine	4.00	-0.59	0.000	-0.41	0.007	↓	↓
Uridine	5.91	-0.68	0.000	-0.40	0.079	↓	↓
Uridine	5.93	-0.61	0.000	-0.34	0.088	↓	↓
Uridine	7.88	-0.65	0.000	-0.33	0.006	↓	↓
Fumarate	6.53	-0.54	0.000	-0.55	0.004	↓	↓
Histidine	7.07	-0.51	0.000	-0.40	0.008	↓	↓
Histidine	7.79	-0.55	0.000	-0.31	0.070	↓	↓
Unk	7.16	-0.35	0.000	-0.60	0.001	↓	↓
Unk	7.37	-0.36	0.000	-0.61	0.010	↓	↓
Phenylalanine	7.38	-0.51	0.000	-0.57	0.001	↓	↓
Metabolites shared between BCT-IOXRT (B) and AMP (B)							
Methanol	3.37	0.38	0.000	0.58	0.001	↑	↑

 doi:10.20944/preprints202603.0491.v1

Unk / Xanthine	7.89	0.48	0.000	0.42	0.049	↑	↑

Legend: Unk – unknown signal; MULTI - overlap signals from more than two metabolites; 2-HB – 2-hydroxybutyrate; 2-HV – 2-hydroxyvalerate; * - glucose has more than a dozen signals in 1H NMR spectra, most of them overlap with each other or with other metabolites, the signal at 5.25 ppm does not overlap with any other signals and thus presents the highest quantification accuracy for glucose.

Discussion

In the present study NMR-based metabolomic analysis of postoperative wound fluids collected from BC patients, with a focus on those treated with intraoperative radiation therapy.

In the 1H NMR spectra (110 samples), 91 signals from 42 metabolites were positively identified, 4 metabolites (5 NMR signals) were annotated as probable, 5 NMR signals were identified as originating from more than one metabolite, and 13 NMR signals remained unknown (Table 3). Multivariate analyzes of the spectroscopic data were carried out using unsupervised PCA to evaluate the distribution of variance in the data and PLS-DA, and its orthogonal equivalent OPLS-DA for class discrimination.

1H NMR allows one to detect circulating blood metabolites and lipoproteins that not only reflect tumour metabolism, but also provide a systemic picture of the balance between tumour and host metabolism. This is due to the fact that each BC patient has a unique set of physiological and immunological conditions. As demonstrated by Derveaux et al., surgical removal of a tumor (lung cancer) causes significant metabolic changes in plasma, indicating that the serum metabolic profile is determined by the presence of the tumor rather than donor-specific characteristics (Derveaux et al., 2023). The levels of several circulating amino acids and glycoproteins, as well as lipoproteins, have already been shown to undergo statistically significant changes in patients with BC. This suggests that disruption of energy homeostasis and amino acid metabolism may facilitate cancer growth and evolution (Cala et al. 2018; Lecuyer et al. 2018). Jobard et al. (2021) reported in a cohort of 791 cases of breast cancer and 791 matched controls that alterations in circulating plasma metabolites were observed even before breast cancer. However, the observed differences were only statistically significant in the premenopausal subgroup. In their previous study, Jobard et al. documented metabolic alterations associated with advanced metastatic breast cancer compared to early local disease (Jobard et al., 2014). Tenori et al. similarly demonstrated that serum NMR spectra can differentiate between early and metastatic breast cancer patients and predict disease recurrence (Tenori et al., 2015). Thus, it shows that NMR is a powerful tool for studying cancer metabolism.

Our findings indicate substantial temporal alterations in metabolic profiles between the time points A and B in both the BCT-IOXRT and AMP groups. These alterations underscore the dynamic changes in the tumour microenvironment following surgical intervention. In the BCT-IOXRT group, a significant decrease in the branched-chain amino acids (valine, isoleucine, and leucine), asparagine, methionine, and glutamate was observed along with the elevated levels of glucose, lactate, and pyruvate. The observed metabolic changes are characteristic of metabolic reprogramming, where decreased levels of essential amino acids such as valine, isoleucine, leucine, and methionine are associated with suppressed growth and induced apoptosis, while elevated glucose, pyruvate, and lactate are part of the Warburg effect, supporting the high biosynthetic and energy needs of cancer cells. Previous studies by Zalewska et al. (2016, 2017) and Kulcenty et al. (2018) demonstrated that IORT-conditioned fluid reduces the population of stem-like cancer cells and activates apoptotic pathways. Branched-chain amino acids are imperative for protein synthesis and activation of signaling pathways such as mTOR, which regulate cancer cell growth. The excessive use of these proteins by cancer cells has been shown to promote proliferation and resistance to treatment.

Xu et al. (2025) emphasize that branched chain amino acids (BCAAs) are key nutrients that support protein synthesis and regulate cell growth. Research shows that cancer cells use BCAAs in a specific way, as fuel and a regulator of metabolism, which promotes their aggressiveness and survival. BCAAs have been shown to play a dual role as building block and energy sources, influencing pathways that control metabolism and growth. They may also promote resistance to

 doi:10.20944/preprints202603.0491.v1

treatment. Understanding these mechanisms opens the possibility of developing new anticancer therapies targeting BCAA metabolism. Increased glucose, lactate, and pyruvate concentrations after IOXRT indicate activation of aerobic glycolysis (Warburg effect), a hallmark of cancer cells. Lactate is not merely a by-product; it has a signaling function, exerts an influence on the tumor microenvironment, and can modulate the immune response. Al-Malsi et al. (2025) describe lactate as an epigenetic regulator through the induction of histone lactylation, which can influence the expression of genes associated with cancer progression.

The observed metabolic changes may also be indicative of immune system activation, consistent with the concept of the abscopal effect described by Jeibouei et al. (2022). Increased levels of lactate and pyruvate have been observed to be associated with immune cell recruitment and remodeling of the tumor microenvironment. The literature supports that intraoperative radiotherapy (IORT) modulates microRNA (miRNA) expression, such as miR-21 and miR-155, which influences immune responses by altering tumor-supportive healing and reshaping local immune signaling (Zalewska et al., 2017).

Decreased levels of glutamate and methionine may indicate reduced biosynthesis activity and altered redox homeostasis. Glutamate is essential for cancer cell proliferation and immune cell function, while methionine is involved in DNA methylation and regulation of gene expression.

According to Liu et al. (2025), disturbances in glutamate and methionine metabolism are characteristic of various breast cancer subtypes and may represent a therapeutic target.

The decreases in ketone bodies, such as 3-hydroxybutyrate and acetoacetate, can indicate changes in energy metabolism and oxidative stress. Their levels correlate with the patient's response to chemotherapy and nutritional status, where their NMR levels serve as a measure of the patient's nutritional status and can indicate the body's response to starvation (Boguszewicz et al., 2024). In the context of breast surgery, patients are required to fast for a period of 24 hours. However, more research is needed to determine whether this relatively brief fasting period will be reflected in postoperative wound fluid.

A decrease in creatine and an increase in creatinine can indicate altered phosphagen metabolism and cellular stress. Creatine acts as an energy buffer and disturbances in creatine levels are observed in many cancers, including breast cancer. An et al. (2022) demonstrated through a proteomic-metabolomic analysis that creatinine and glutamate are among 47 metabolites that have a high diagnostic value for breast cancer.

In the review by Vignoli et al. (Vignoli, 2021), various applications of NMR-based metabolomics are gathered, demonstrating that this approach is optimal for BC cancer research, in particular for prognostic and stratification purposes. This review focuses on the biochemical characterization and stratification of breast cancer patients using different biospecies: breast tissue, blood serum/plasma, and urine. NMR-based metabolomic studies in serum blood samples are worth mentioning. Jobard et al. (2014) and Tenori et al. (2015) found that specific blood metabolites differ between early-stage and metastatic breast cancer; later, Hart et al. (Hart, 2017) reported that preoperative serum metabolomic profiles can be prognostic for disease recurrence and long-term BC risk (Lecuyer et al., 2018). Breast cancer and healthy subjects were also shown to be discriminated by NMR (Cala et al., 2018). Finally, Jobard et al. (Jobard et al., 2021) showed that non-targeted plasma NMR metabolomics can predict the risk of breast cancer in premenopausal women. However, in the reviewed review mentioned, BC surgical wound fluids were not analyzed, therefore, the current effort is the first to examine the metabolic profiles of WF. The metabolic information is particularly important because these fluids may reflect the inflammation and aggressiveness of breast cancers (Agresti et al. 2019). Furthermore, insight into their metabolic changes can serve as a source of predictive biomarkers (Hartman et al., 2021).

Our study confirms also the observations by Wuhrer et al. (2021) that the postoperative fluids from the patients treated with intraoperative radiotherapy may have a different composition than those from patients who did not receive IORT (Wuhrer et al. 2021).

 doi:10.20944/preprints202603.0491.v1

Conclusions

The objective of the present study was to perform a metabolomic analysis of postoperative fluids in patients with breast cancer who underwent breast preservation surgery with X-rays intraoperative radiation therapy (IOXRT) and mastectomy (AMP). 1H NMR spectroscopy was utilized to identify and quantify metabolites in the spectra. The results of PCA, PLS-DA, and OPLS-DA demonstrated clear disparities between the samples collected on the first and fifth days after surgery in both groups. However, in general no significant differences were observed between the BCT-IOXRT and AMP groups. In the BCT-IOXRT group, a decrease in amino acids such as valine, isoleucine, asparagine, and lysine was observed, along with an increase in glycolysis-related metabolites, including lactate and pyruvate. In the AMP group, there were characteristic changes in 2-oxoglutarate and hypoxanthine levels and an increase in glucose and creatinine at a later time. A common trend observed in both groups was a decrease in signals from the ketone bodies, including 3-hydroxybutyrate, acetone, and acetoacetate, along with methionine. The results indicate that postoperative fluids exhibit significant biological properties and differences in metabolite profiles depending on the type of treatment, and that IOXRT affects the metabolism of cancer cells by intensifying glycolytic processes and apoptosis.

Metabolomic analysis of postoperative fluids has the potential to serve as a prognostic tool, offering information on response to treatment and facilitating a more comprehensive understanding of the dynamic interactions between the tumor microenvironment and the therapeutic modalities used.

Limitations and Future Directions

The authors of the study are aware of a number of limitations of this study, but due to its pilot nature and the innovative research approach, it was decided to publish the preliminary conclusions. First, the limited sample size of the study group (particularly patients with AMP) can compromise the statistical power and generalizability of the results. The OPLS-DA models that compared the BCT-IOXRT and AMP groups did not meet the statistical significance criteria, which limits the possibility of drawing conclusions about the impact of the type of treatment on the metabolome in the intergroup comparison. Due to the recent nature of the study, long-term clinical outcomes (eg, recurrence, survival) were not included, making it difficult to assess whether metabolomic changes have real prognostic significance. This study focuses exclusively on metabolomics, a field that limits a full understanding of biological mechanisms. This preliminary analysis did not include information on diet, medications or the metabolic status of patients, which can affect the composition of postoperative fluid. In light of these limitations, the study's subsequent phase will involve an increase in the number of patients, along with the potential for conducting an analysis on a control group (e.g., patients who have undergone surgery for benign breast lesions). This approach aims to enhance the study's understanding of the impact of cancer on fluid composition. The objective of this study is to integrate metabolomics with proteomics, transcriptomics, and microRNA analysis. The incorporation of long-term clinical data at this stage is particularly challenging, as the 10-year survival rate for early-stage breast cancer is 96%. However, an effort will be made to establish a correlation between metabolomic alterations and clinical outcomes, with the objective of evaluating their prognostic significance. In the subsequent phases of the study, standardization and control of confounders (data on diet, medications, metabolic status, and lifestyle) will be incorporated.

Author Contributions: Concept: A.GK., J.W; Methodology: A.GK.; Ł.B., A.S., M.C., M.TA, M.K., B.ŁS. Software: Ł.B., A.S., M.C.; Validation: A.S., M.C., M.K., B.ŁS; Formal analysis: Ł.B., A.S., M.C. Research: A.GK., Ł.B., A.S., M.C; Resources, Ł.B..; Data curation, Writing – preparation of the original draft, A.GK, J.W., Ł.B.; Writing – review and editing, A.GK., Ł.B., M.S., J.W.; Visualization, Ł.B., A.GK.,. Supervision, M.S., J.W; Project administration, A.GK.

Funding: No funding.

 doi:10.20944/preprints202603.0491.v1

Conflicts of Interest: The authors declare that there is no conflict of interest.

Ethical Declaration: The authors declare that the use of samples from breast cancer patients CONFIRMS that all experiments were conducted in accordance with the relevant guidelines and regulations. The authors confirm that all methods were performed in accordance with the relevant guidelines and regulations. The authors confirm that all experimental protocols were approved by the Bioethics Committee. The study was approved by the Bioethics Committee of the Maria Skłodowska-Curie National Research Institute of Oncology, Gliwice Branch (No. KB/430-29/23, approved on March 16, 2023).

Final Remarks: All data (anonymized) are available from the authors and can be made available to anyone interested. To access the data, please send a request to Dr. Łukasz Boguszewicz.

References

Bala L, Sharma A, Yellapa RK, Roy R, Choudhuri G, Khetrapal CL. ^{1}H NMR spectroscopy of ascitic fluid: discrimination between malignant and benign ascites and comparison with conventional methods. Journal of Magnetic Resonance in Biomedicine 21, 606–614 (2008). https://doi.org/10.1002/nbm.1232

Beckonert O, Keun HC, Ebbels TM, Bundy J, Holmes E, Lindon JC, Nicholson JK. Metabolic profiling, metabolomic and metabonomic procedures for NMR spectroscopy of urine, plasma, serum and tissue extracts. Nature Protocols 2, 2692–2703 (2007). https://doi.org/10.1038/nprot.2007.376

Belletti B, Vaidya JS, D'Andrea S, Entschladen F, Roncadin M, Lovat F, Berton S, Perin T, Candiani E, Reccanello S. Targeted intraoperative radiotherapy impairs the stimulation of breast cancer cell proliferation and invasion caused by surgical wounding. Clinical Cancer Research 14, 1325–1332 (2008). https://doi.org/10.1158/1078-0432.CCR-07-4483

Boguszewicz Ł, Bieleń A, Jarczewski JD, Ciszek M, Skorupa A, Składowski K, Sokół M. Molecular response to induction chemotherapy and its correlation with treatment outcome in head and neck cancer patients by means of NMR-based metabolomics. BMC Cancer 21, 410 (2021).
https://doi.org/10.1186/s12885-021-08137-4

Boguszewicz Ł, Bieleń A, Ciszek M, Skorupa A, Mrochem-Kwarciak J, Składowski K, Sokół M. Metabolomic Insight into Implications of Induction Chemotherapy Followed by Concomitant Chemoradiotherapy in Locally Advanced Head and Neck Cancer. Int J Mol Sci. 2023 Dec 22;25(1):188. doi: 10.3390/ijms25010188. PMID: 38203359; PMCID: PMC10779362.

Boguszewicz Ł, Bieleń A, Jarczewski JD, Ciszek M, Skorupa A, Mrochem-Kwarciak J, Składowski K, Sokół M. NMR-based metabolomics of blood serum in predicting response to induction chemotherapy in head and neck cancer. International Journal of Molecular Sciences 25, 7555 (2024). https://doi.org/10.3390/ijms25147555

Bray F, Laversanne M, Sung H, Ferlay J, Siegel RL, Soerjomataram I, Jemal A. Global cancer statistics 2022: GLOBOCAN estimates of incidence and mortality worldwide for 36 cancers in 185 countries. CA: A Cancer Journal for Clinicians 74, 229–263 (2024). https://doi.org/10.3322/caac.21820

Chae EY, Shin HJ, Kim S, Baek HM, Yoon D, Kim S, Shim YE, Kim HH, Cha JH, Choi WJ. The role of high-resolution magic angle spinning ^{1}H NMR spectroscopy for predicting the invasive component in ductal carcinoma in situ. PLoS ONE 11, e0161038 (2016). https://doi.org/10.1371/journal.pone.0161038

Donker M, Litière S, Werutsky G, Julien JP, Fentiman IS, Agresti R, Rouanet P, de Lara CT, Bartelink H, Duez N, Rutgers EJ, Bijker N. Breast-conserving treatment with or without radiotherapy in ductal carcinoma in situ: 15-year recurrence rates from the EORTC 10853 trial. Journal of Clinical Oncology 31, 4054–4059 (2013). https://doi.org/10.1200/JCO.2013.49.5077

Giskeødegård GF, Madssen TS, Euceda LR, Bathen TF. NMR-based metabolomics of biofluids in cancer. NMR in Biomedicine 32, e3927 (2018). https://doi.org/10.1002/nbm.3927

Gogiashvili M, Nowacki J, Hergenröder R, Hengstler JG, Lambert J, Edlund K. HR-MAS NMR based quantitative metabolomics in breast cancer. Metabolites 9, 19 (2019). https://doi.org/10.3390/metabo9020019

Jeibouei S, Shams F, Mohebichamkhorami F, Sanooghi D, Faal B, Akbari ME, Zali H. Biological and clinical review of IORT-induced wound fluid in breast cancer patients. Frontiers in Oncology 12, 980513 (2022). https://doi.org/10.3389/fonc.2022.980513

 doi:10.20944/preprints202603.0491.v1

Junka A, Wojtowicz W, Ząbek A, Krasowski G, Smutnicka D, Bakalorz B, Boruta A, Dziadas M, Młynarz P, Sedghizadeh PP, Bartoszewicz M. Metabolic profiles of exudates from chronic leg ulcerations. Journal of Pharmaceutical and Biomedical Analysis 137, 13–22 (2017). https://doi.org/10.1016/j.jpba.2017.01.018

Kulcenty KI, Piotrowski I, Zaleska K, Murawa D, Suchorska WM. Wound fluids collected after IORT activate the extrinsic apoptotic pathway in MCF7 cells. Ginekologia Polska 89, 175–182 (2018). https://doi.org/10.5603/GP.a2018.0030

Maria RM, Altei WF, Andricopulo AD, Becceneri AB, Cominetti MR, Venâncio T, Colnago LA. Characterization of metabolic profile of intact breast cells by HR-MAS NMR. Analytical Biochemistry 488, 14–18 (2015). https://doi.org/10.1016/j.ab.2015.07.015

Maria RM, Altei WF, Selistre-de-Araujo HS, Colnago LA. Effects of doxorubicin, cisplatin and tamoxifen on metabolic profile of MCF-7 cells by HR-MAS NMR. Biochemistry 56, 2219–2224 (2017). https://doi.org/10.1021/acs.biochem.7b00088

McCready DR, Hanna W, Kahn H, Chapman JA, Wall J, Fish EB, Lickley HL. Factors associated with local breast cancer recurrence after lumpectomy alone. Annals of Surgical Oncology 3, 358–366 (1996). https://doi.org/10.1007/BF02305771

Piroth MD, Strnad V, Krug D, Fastner G, Baumann R, Combs SE, Duma MN, Dunst J, Feyer P, Fietkau R, Haase W, Harms W, Hehr T, Sedlmayer F, Souchon R, Budach W. Long-term results of the TARGIT-A trial: More questions than answers. Breast Care 17, 81–84 (2022). https://doi.org/10.1159/000521754

Silva C, Perestrelo R, Silva P, Tomás H, Câmara JS. Breast cancer metabolomics: from analytical platforms to multivariate data analysis. Metabolites 9, 102 (2019). https://doi.org/10.3390/metabo9050102

Skorupa A, Ciszek M, Turska-d'Amico M, Stobiecka E, Chmielik E, Szumniak R, d'Amico A, Boguszewicz Ł, Sokół M. The relationship between histological composition and metabolic profile in breast tumors and peritumoral tissue determined with ^{1}H HR-MAS NMR spectroscopy. Cancers 15, 1283 (2023). https://doi.org/10.3390/cancers15041283

Sung H, Ferlay J, Siegel RL, Laversanne M, Soerjomataram I, Jemal A, Bray F. Global cancer statistics 2020: GLOBOCAN estimates of incidence and mortality worldwide. CA: A Cancer Journal for Clinicians 71, 209–249 (2021). https://doi.org/10.3322/caac.21660

Troester MA, Lee MH, Carter M, Fan C, Cowan DW, Perez ER, Pirone JR, Perou CM, Jerry DJ, Schneider SS. Activation of host wound responses in breast cancer microenvironment. Clinical Cancer Research 15, 7020–7028 (2009). https://doi.org/10.1158/1078-0432.CCR-09-1149

Vaidya JS, Baum M, Tobias J, D'Souza D, Naidu S, Morgan S, Metaxas M, Harte K, Sliski A, Thomson E. Targeted intra-operative radiotherapy (TARGIT): an innovative method for early breast cancer. Annals of Oncology 12, 1075–1080 (2001). https://doi.org/10.1023/A:1011624629738

Vaidya JS, Wenz F, Bulsara M, Tobias JS, Joseph DJ, Keshtgar M, Flyger HL, Massarut S, Alvarado M, Saunders C, et al. Risk-adapted targeted intraoperative radiotherapy versus whole-breast radiotherapy: 5-year results of the TARGIT-A trial. The Lancet 383, 603–613 (2014). https://doi.org/10.1016/S0140-6736(13)61950-9

Veronesi U, Orecchia R, Maisonneuve P, Viale G, Rotmensz N, Sangalli C, Luini A, Veronesi P, Galimberti V, Zurrida S. Intraoperative radiotherapy versus external radiotherapy for early breast cancer (ELIOT): a randomised controlled equivalence trial. The Lancet Oncology 14, 1269–1277 (2013). https://doi.org/10.1016/S1470-2045(13)70497-2

Vignoli A, Risi E, McCartney A, Migliaccio I, Moretti E, Malorni L, Luchinat C, Biganzoli L, Tenori L. Precision oncology via NMR-based metabolomics: a review on breast cancer. International Journal of Molecular Sciences 22, 4687 (2021). https://doi.org/10.3390/ijms22094687

Wiklund S, Johansson E, Sjöström L, Mellerowicz EJ, Edlund U, Shockcor JP, Gottfries J, Moritz T, Trygg J. Visualization of GC/TOF-MS-based metabolomics data using OPLS class models. Analytical Chemistry 80, 115–122 (2008). https://doi.org/10.1021/ac0713510

Wydmański J, Miszczyk L, Suwiński R, Mąka B, Orlef A, Bekman A, Maciejewski B. A new method of targeted intraoperative radiotherapy using the orthovoltage photon radiosurgery system. Nowotwory Journal of Oncology 55, 320 (2005).

 doi:10.20944/preprints202603.0491.v1

Zaleska K, Suchorska WM, Przybyła A, Murawa D. Effect of surgical wound fluids after IORT on the cancer stem cell phenotype in human breast cancer cell lines. Oncology Letters 12, 3707–3714 (2016). https://doi.org/10.3892/ol.2016.5104

Zaleska K, Przybyła A, Kulcenty K, Wichtowski M, Mackiewicz A, Suchorska W, Murawa D. Wound fluids affect miR-21, miR-155 and miR-221 expression in breast cancer cell lines; effect partially abrogated by IORT. Oncology Letters 14, 4029–4036 (2017). https://doi.org/10.3892/ol.2017.6628